Analyst

RSC Publishing

PAPER

View Article Online
View Journal | View Issue

The characterization of normal thyroid tissue by micro-FTIR spectroscopy

Cite this: *Analyst*, 2013, **138**, 7094

Thiago M. Pereira,[ab] Denise M. Zezell,*[a] Benjamin Bird,[b] Milos Miljković[b] and Max Diem[b]

Received 9th February 2013
Accepted 14th July 2013

DOI: 10.1039/c3an00296a

www.rsc.org/analyst

In this paper, we report the spectral patterns of normal human thyroid tissue and methodology to interpret hyperspectral imaging data and protein conformational changes observed therein. Raw image datasets were imported into software written in-house in the MATLAB environment and processed to yield pseudo-color images of the tissue sections. All spectra were vector normalized, noise-filtered, and corrected for water-vapour contributions and scattering effects before being subjected to Hierarchical Cluster Analysis (HCA) and correlated with histological structures obtained from images of H&E-stained parallel tissue sections. We successfully identified a protein structural heterogeneity that can be correlated with the spatially resolved amount of iodine in the thyroglobulin structure of colloids and follicular cells.

Introduction

The thyroid gland is one of the most important glands of the endocrine system and secretes mainly two hormones (triiodothyronine and thyroxine) that are required for many physiological processes such as homeostasis, normal growth and energy production.[1] Because of this, the thyroid gland is very sensitive and in a constant state of adaptation. For example, during pregnancy, lactation, puberty and similar states of psychological stress, the gland becomes larger and more active; also, the follicle cells become larger and more columnar. When the stress subsides, involution of the gland occurs, and the follicular cells regain their normal shape.[2,3]

Anatomically, the thyroid gland consists of a thin layer of epithelial cells (follicular cells) that produce the precursor of the thyroid hormones, thyroglobulin, which is stored in structures known as colloids until they are needed by the body.[4] Thyroglobulin is a glycoprotein and, aside from being the precursor of the hormones, its main function is to store the iodine, and T3 (triiodothyronine) and T4 (thyroxine) hormones.[5,6] The synthesis of thyroglobulin is a very complex process and can be divided into 4 steps: protein synthesis, glycosylation, iodination and conjugation. The first two steps occur inside the follicular cells while the last two occur in the colloid.

Numerous studies[7–10] have shown that spectral histopathology (SHP),[9,11,12] the combination of infrared spectral imaging, multivariate analysis and information from classical pathology, can detect, diagnose and analyze diseases based on the observation of compositional changes occurring in small tissues that accompany disease.[13] SHP represents a different approach to the analysis of tissue and cells than classical histopathology that uses visible light and the human eye to detect morphological changes in the tissue. In the present paper, SHP is used to monitor complex biochemical processes in healthy thyroid tissue, rather than detecting or diagnosing disease.

There are several studies[14–16] using FTIR to classify and biochemically characterize thyroid tissue. However, these studies were focused primarily on the biochemical differences among normal and abnormal stages of disease. These studies were also not performed using micro-FTIR techniques and hence the accurate biochemical characterization of each thyroid specific cell type was not performed. The complete biochemical characterization of these thyroid tissue types is of great importance since it can reveal a clearer picture of aberrant sequences in early stage thyroid disease that cannot presently be observed by classical histopathology.

Healthy thyroid tissue is an ideal system to explore the biostructural capabilities of SHP. The biochemical processing steps from thyroglobulin to its iodinated state can be detected by SHP and interpreted in terms of known biochemical steps. This report presents a detailed insight into the structural sensitivity of SHP toward subtle conformational changes that occur within the colloids of normal thyroid tissue.

[a]*Centro de Lasers e Aplicações, Instituto de Pesquisas Energéticas e Nucleares, Avenida Professor Lineu Prestes 2242, 05508-000, São Paulo, SP, Brazil. E-mail: zezell@usp.br; Fax: +55 (11)3133-9375; Tel: +55 (11)3133-9370*

[b]*Laboratory for Spectral Diagnosis (LSpD), Department of Chemistry and Chemical Biology, Northeastern University, 360 Huntington Avenue, Boston, USA. E-mail: m.diem@neu.edu; Fax: +1 (617)373-7773; Tel: +1 (617)373-5099*

The complex hormonal action can be disrupted if the gland itself is injured or affected by diseases such as neoplasia.[2,17] As a consequence the equilibrium inside the thyroid follicle is altered. The gland can produce high amounts of hormone (hyperthyroidism) or low amounts of hormone (hypothyroidism). These abnormal aberrations in hormone production can lead to several serious health problems. Therefore, it is important to develop new methods to characterize the thyroid follicle in order to evaluate the normal and abnormal physiological process.

Fine needle aspiration (FNA) is one of the most common procedures for diagnosis of thyroid disorders. However, this method presents a high rate of false-negative diagnoses (up to 37%)[2] and the differentiation among the common thyroid diseases is quite difficult. The low specificity of thyroid FNA can be inadequate positioning of the needle relative to the lesion, which is guided by palpation, or due to the fact that the aspirate may contain no diseased cells or insufficient amount of them, which does not allow a precise diagnosis. Nevertheless, any residual material of the FNA, such as colloids, contains valuable biochemical information of the thyroid condition[18] that can be analyzed by SHP and give more biochemical information for better diagnosis.

Thus, the characterization of normal thyroid tissue by micro-FTIR is important since it can report biochemical changes in follicular cells and follicle colloids that may occur before current histological and cytological methods can observe them. The report presented here concentrates on normal thyroid tissue and its biochemical composition.

Materials and methods

Sample preparation

The thyroid tissue microarray (TMA, BiomaxUS, TH804) used in this study contained 80 different patient tissue cores that measure *ca.* 1.5 mm in diameter. The paraffin-embedded tissue sections were microtomed at 5 μm thickness and mounted on slides by the supplier according to our request as described below. One section of each sample was mounted on a glass microscope slide and hematoxylin and eosin (H&E) stained. Two sequential sections were mounted on infrared reflective substrates (Kevley Technologies, Chesterland, OH).

The first H&E stained section was used to localize the anatomical features, and to correlate HCA images that were constructed *via* FTIR analysis on the second unstained and de-paraffinized section. The tissue section on the infrared reflective slide was de-paraffinized and dried before data acquisition. Although only imaging results from one tissue core are reported (Fig. 1), the spectral patterns to be discussed were observed for all normal thyroid tissue cores in the TMA.

Data acquisition

Infrared spectral hypercubes were acquired in transflection mode using an FTIR imaging system (Spectrum 1/Spotlight 400, Perkin Elmer, Shelton, CT) that incorporates a 16 element focal plane array (FPA) detector system. The size of each HgCdTe detector element is 25 μm × 25 μm, and the detector is cooled by liquid nitrogen. Infrared maps were acquired with an image magnification of 4; thus the pixel size covered by each detector was 6.25 μm × 6.25 μm. The images are collected by moving the sample through the focal point of the infrared microscope.

Infrared micro-spectral images were recorded in transflection (transmission/reflection) mode with a pixel size of 6.25 μm × 6.25 μm, a spectral resolution of 4 cm^{-1} and the co-addition of 2 interferograms before Norton–Beer apodization and Fourier transformation. An appropriate background spectrum was collected outside the sample area by the co-addition of 120 interferograms.

The entire instrument and microscope were purged with dry air to keep the relative humidity constant and below 5% to eliminate water vapor contributions to the FTIR spectra.

Data processing and analysis

After elimination of spectra collected from areas where no tissue exists or displays excess noise, the hyperspectral imaging data sets were composed of *ca.* 13 000 spectra, each containing 1625 spectral intensity values between 750 and 4000 cm^{-1}. The datasets were imported into software written in-house in the MATLAB environment. Data pre-processing included the restriction of the wavenumber range between 778 and 1800 cm^{-1}, imposition of selection criteria to avoid pixels not covered by tissue and/or those that displayed excessively strong scattering effects (Amide I peak position <1620 cm^{-1}). All spectra were vector normalized and converted to second derivatives using a Savitzky–Golay smoothing filter (11-point), vector normalised and phase corrected.[19]

Spectral datasets were subsequently converted to pseudo-color images using hierarchical cluster analysis (HCA), which clusters patterns in a dataset based on their spectral similarity. For this purpose the Euclidean distance was used to define the spectral similarity and Ward's algorithm was used for clustering. This process creates pseudo-color images that reproduce stained images very well. Further analysis of spectral data, pre-sorted by HCA, is used to discuss the biochemical characteristics of anatomical structures of normal thyroid tissue.

Hormone measurement

The FTIR spectra of triiodothyronine (T3) and thyroxine (T4) were acquired microscopically in order to identify the contribution of the thyroid hormones to the FTIR spectra in the colloids of normal thyroid patients. The hormones were obtained commercially from Sigma-Aldrich, and were dissolved in distilled water. A drop of solution was spotted onto low-e microscope slides and dried for 24 hours before measurement.

The FTIR measurements were collected in transflection mode using an FTIR imaging system (Spectrum 1/Spotlight 400, Perkin Elmer, Shelton, CT) using the 100 μm diameter single element HgCdTe detector. The spectrum from each hormone was acquired using a 4 cm^{-1} spectral resolution, the co-addition of 1024 interferograms, an aperture of 100 μm × 100 μm, and between 700 cm^{-1} and 4000 cm^{-1}.

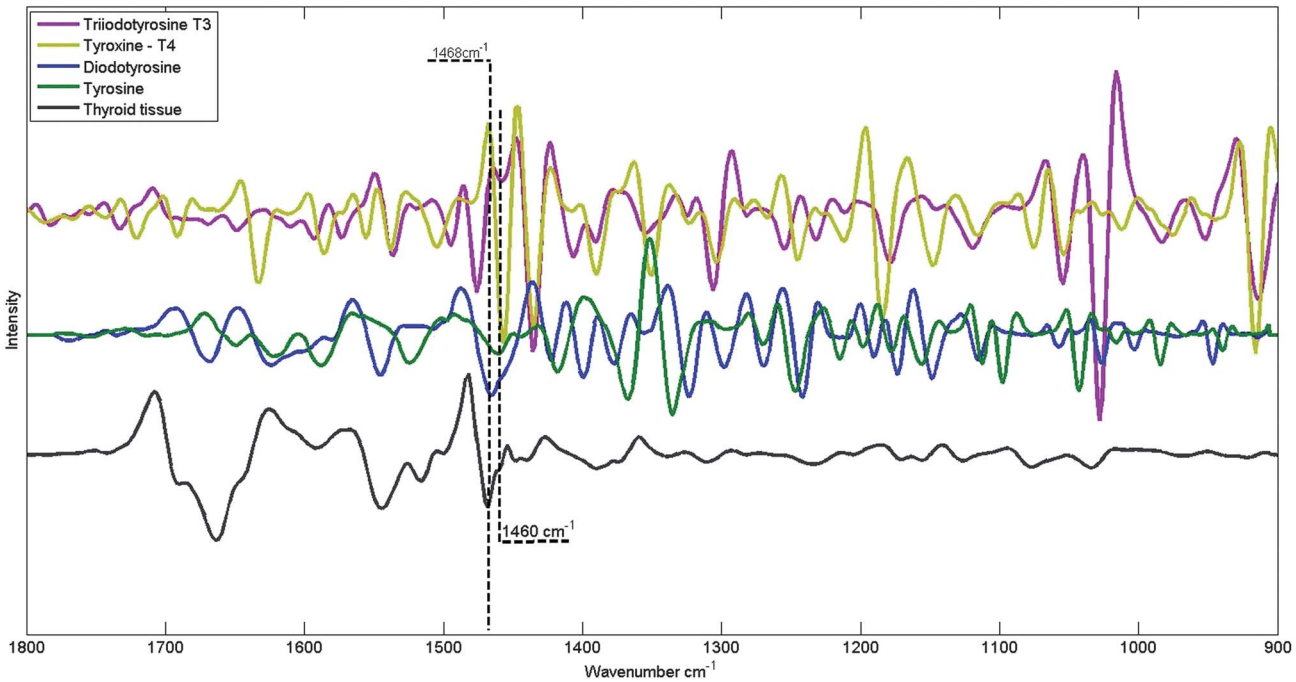

Fig. 1 Second derivative of FTIR spectra of hormones triiodothyronine (T3), thyroxine (T4), diiodotyrosine[20] (1468 cm^{-1}), tyrosine[20] and thyroid tissue.

Results and discussion

Hormones and their precursors

Fig. 1 shows the FTIR spectra of the hormones triiodothyronine (T3), thyroxine (T4), diiodotyrosine and healthy thyroid tissue in the second derivative format.

Fig. 1 shows the 2nd derivative FTIR spectra of the pure thyroid hormones T3 and T4. These spectra exhibit strong peaks at 916, 1630, 1460 1190, 1476, and 1458 cm^{-1} respectively. We conversely observe a strong peak at 1468 cm^{-1} for diiodotyrosine[20] (blue trace). A normal thyroid tissue spectrum is shown for direct comparison (gray trace). While there are several strong peaks related to thyroid hormones and diiodotyrosine in the spectral region 900–1800 cm^{-1}, the most prominent correlation of the hormone and/or its precursors with the thyroid tissue spectrum is the peak located at 1468 cm^{-1} and its low wavenumber shoulder at *ca.* 1460 cm^{-1}.

Fig. 2 shows the triiodothyronine (T3) and thyroxine (T4) molecules that are formed from two phenol groups.

An investigation[21] that utilized density functional theory calculations for thyroid hormones concluded that the spectral band located at 1458 cm^{-1} can be directly correlated with an aromatic ring vibration when one iodine atom is attached to the β phenol ring, and is only observed in the T3 hormone. The β phenol moiety of the T3 molecule is also formed from monoiodotyrosine (MIT) and thus this vibration is also related to MIT.

We conclude that the peak at 1468 cm^{-1} observed in our results is related to the amount of diiodotyrosine (DIT) and the shape of this peak is quite similar to that of normal thyroid tissue. The shoulder (1460 cm^{-1}) is related to MIT.

DIT and MIT are hormone precursors and are formed in the colloids when the phenol group[1] of the tyrosine amino acid from the thyroglobulin molecule is iodinated at position 3 and/or 5 of the aromatic ring. We believe we do not observe any distinct peaks associated with the thyroid hormone in tissue spectra since the amount of DIT and MIT is approximately 6 times larger than thyroid hormones in the phenol residual sites of thyroglobulin.[22] We found the peak at 1468 cm^{-1} and a shoulder at 1460 cm^{-1} in all mean spectra from the normal thyroid tissue and they never shifted, but showed differences in their intensity profile.

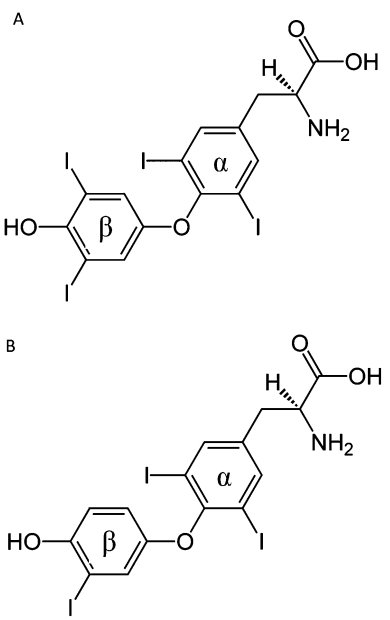

Fig. 2 Structure of the thyroid hormone triiodothyronine (T3) and thyroxine (T4).

This peak (1468 cm^{-1}) and its low wavenumber shoulder (1460 cm^{-1}) show the amount of iodine linked to the thyroglobulin molecule. When consulting literature[22–25] addressing quantitative iodine measurement in the thyroid, we observed that the investigation that was performed used elementary quantitative analysis and thus did not distinguish whether or not iodine is attached to the thyroglobulin molecule. To the best of our knowledge, our investigation is the first to report the semi-quantitative spatially resolved measurement of iodine content linked to thyroglobulin.

Thyroid tissue

Fig. 3 shows spectral images, constructed *via* HCA (Panels A and B), a univariate plot of the intensity at 1468 cm^{-1} (Panel C) and a visual image of the parallel stained tissue section (Panel D).

The nine-cluster image in Fig. 3A (cluster image constructed from the 900–1800 cm^{-1} spectral range) reveals the follicular cells as a red colored cluster, and the colloid represented by green, pink and cyan colored clusters. The chemical composition in the colloid areas of different colors is quite different, as will be discussed below. Most likely, the red cluster in Fig. 3A is not due to follicular cells only, but it seems that pixels of follicular cells and the innermost layer of the colloid are mixed. This observation is not attributed to scattering effects that are often observed for small, cellular structures, since the cells are embedded in the glycoproteins of the colloid, and thus are not exposed to large changes in refractive index that can give rise to these confounding effects. Rather, we believe that the width of the red areas reflects the similarity between the glycoprotein produced by the follicular cells and that stored in the innermost layers in the colloid.

As was found in earlier work on lymph node SHP,[13] when selecting a specific spectral region without amide contribution, biochemical differences can be emphasized for three reasons. First, the spectra were corrected for dispersive line shapes by a phase correction algorithm that has been demonstrated to remove scattering effects satisfactorily.[26] Second, the observed heterogeneity of the protein spectra is enormous (see Fig. 4); thus, by cutting the spectral range to exclude most of the protein heterogeneity, only small differences between spectra of pure follicular cells are observed and thus the colloid directly surrounding them can be emphasized. Third, the follicular cells are embedded in the colloid and therefore, their refractive index is matched with their surroundings. Nevertheless, the follicular cells are best resolved in the 900–1358 cm^{-1} range but their position is not markedly different from that indicated by the entire spectral range.

Panel B of Fig. 3 depicts a nine-cluster image constructed from the 900–1350 cm^{-1} spectral range. This image shows a better definition of areas of follicular cells (in red), and also of the onion shell-like structure of some colloids. The colloid marked by the white arrow in Fig. 3B, for example, shows different layers in the visible as well as in the HCA images, but these differences are better defined in Panel 3B. This colloid, for example, is made up of 3 clusters while others are composed of one cluster only. At this point, we can interpret the different colloid spectral properties (see below), but do not have any explanation about the biological meaning of these differences.

Fig. 3C shows an intensity image constructed using the spectral band located at 1468 cm^{-1}, since this peak can be directly associated with iodine in the thyroglobulin structure. Lighter grey areas of colloids represent lower content of iodinated thyroglobulin. Using this image we can further observe that the amount of iodine has a strong relationship with colloid clusters (grey, dark green and cyan). To the best of our knowledge, this is the first report in the literature that shows a microscopic image of the iodine content linked to thyroglobulin. This result is important since in many thyroid disorders,

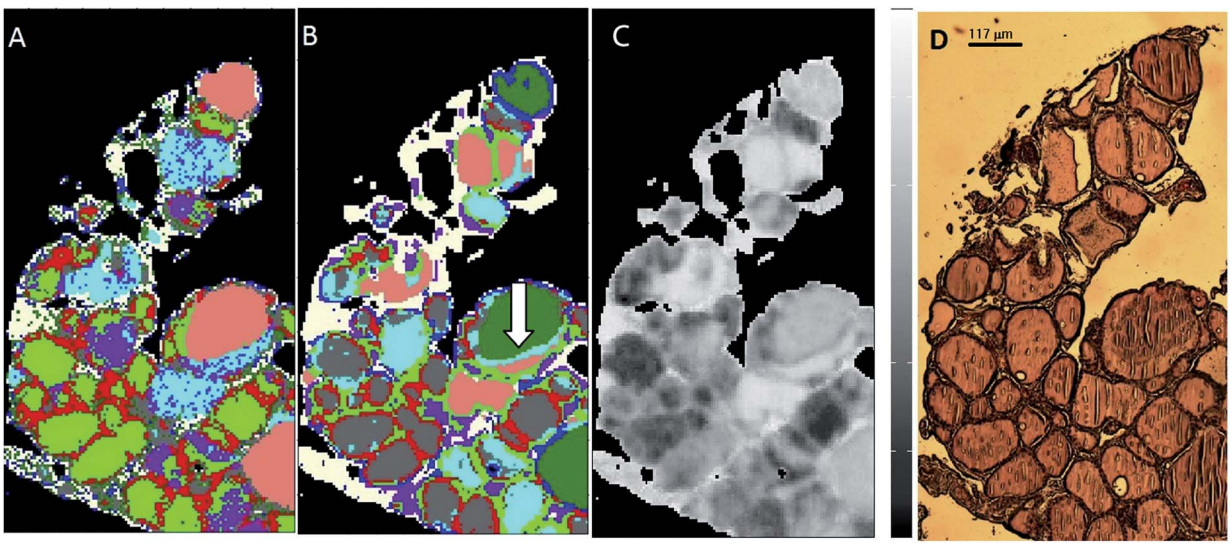

Fig. 3 Panel A: 9-cluster spectral image, constructed *via* HCA from the 900–1800 cm^{-1} spectral range. (B) 9-Cluster image constructed from the 900–1350 cm^{-1} spectral range. (C) Univariate display of the intensity at 1468 cm^{-1} (darker gray corresponds to higher intensity). (D) Visual image of the parallel H&E-stained tissue core.

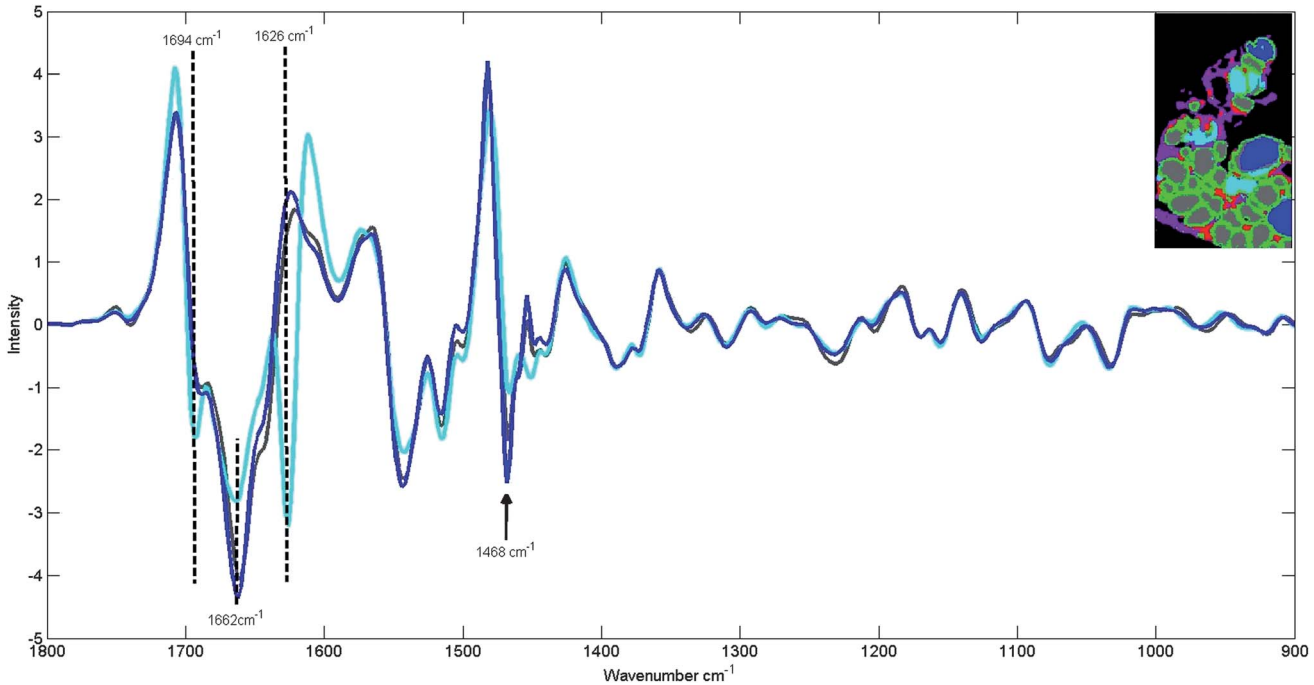

Fig. 4 Mean 2nd derivative spectra from colloid regions, obtained from the 6-clustered spectral image (upper right) which was constructed *via* HCA from the 900–1350 cm^{-1} spectral range. Colors in the second derivative spectra correspond to the same color of the cluster at the upper right figure.

such as goiter, the amount of iodine plays a key role in the early development of these diseases.

We also observed very large protein heterogeneity in the colloids of the thyroid that came as quite a surprise at first, and requires a more detailed understanding of the biochemical processes and protein structural changes within the colloid. Furthermore, thyroid disorders such as goiter and papillary carcinoma occur in follicular cells, but also influence the properties of the thyroglobulin proteins. A detailed understanding of the protein spectral changes can shed light on the

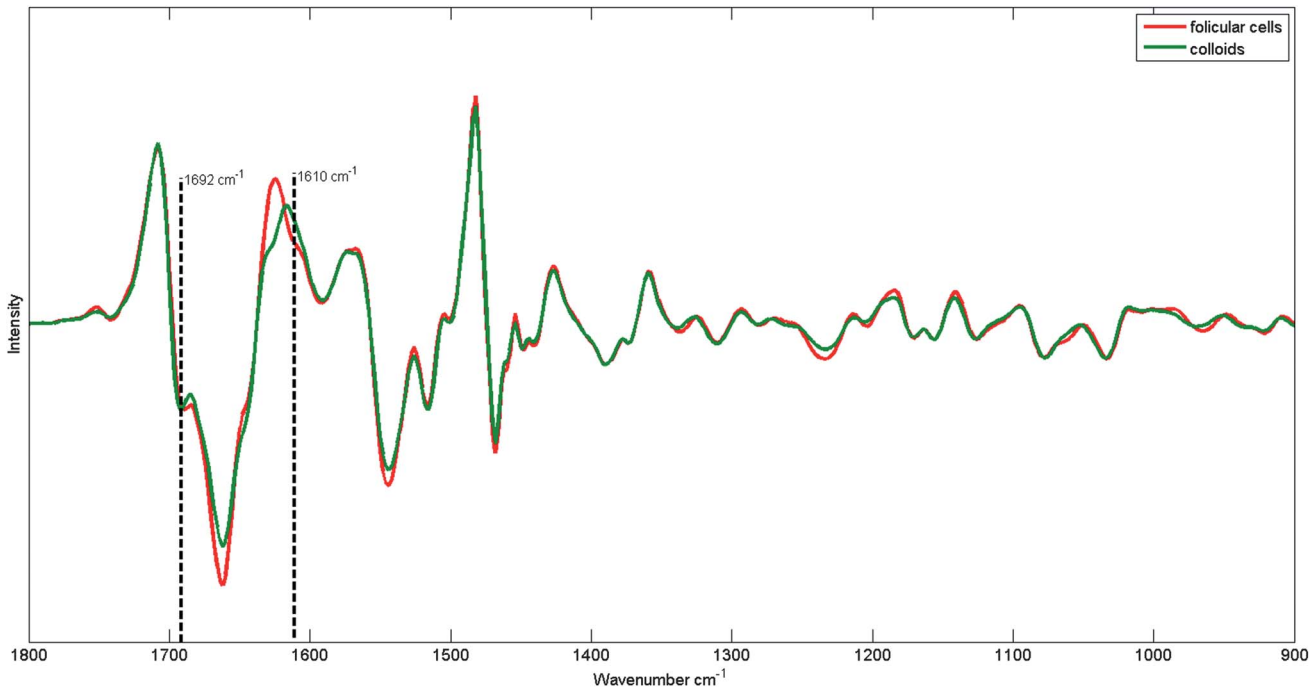

Fig. 5 Comparison of mean 2nd derivative spectra of follicular cells (red line, corresponding to the red cluster in Fig. 3B) and adjacent colloid (green line, corresponding to the dark green, grey and cyan colloid clusters of Fig. 3B).

physiological process inside the follicular cells because synthesis and glycosylation of thyroglobulin occur inside these cells.

Fig. 4 shows the 2nd derivative mean cluster spectra of the colloid regions. The biggest differences between these spectra are found in the amide I region. The grey and dark blue (pink, dark green and white clusters in Fig. 3B) traces are mostly due to α-helical proteins, while the cyan trace (grey and cyan clusters in Fig. 3B) in Fig. 4 exhibits typical β-sheet structure markers at 1694 cm^{-1} and 1628 cm^{-1}. These spectral patterns suggest that the colloid proteins have two different conformations: α-helix and β-sheet.

Inspection of the spectral traces in Fig. 4 reveals that spectral differences in the amide I region present direct relationship with the peak at 1468 cm^{-1}. This fact is evidence for the iodization process, and possibly the linkage of the second aromatic ring to the β-tyrosine residue.

It has been shown[27] that the thyroglobulin from humans has two distinct conformations: one is highly structured (high alpha-helix content), which contains the hormonogenic (iodine content) sites, while the other is less structured.

Thyroglobulin, which has tyrosine-rich proteins, is produced by follicular cells and is stored in the colloid. In the colloid, both positions one and/or two that are adjacent to the OH functional group in tyrosine are iodinated and form monoiodotyrosine (MIT) and diiodotyrosine (DIT) respectively. Subsequently, another iodinated tyrosine is linked to form triiodothyronine (MIT and DIT) or thyroxine (DIT and DIT).[1] Thus, the iodinated thyroglobulin re-enters the follicular cells where the hormones T3 and T4 are split from the protein backbone.

We conclude that the cyan cluster in Fig. 3B is due to the non-iodinated form of thyroglobulin shown in lighter gray in Panel 3C, which has a β-sheet conformation, while the grey and blue clusters in Fig. 3B are due to areas of high amounts of iodine, namely the iodinated form of thyroglobulin that has an α-helical conformation. The spectral signatures of the other thyroid hormone, triiodothyronine T3 are not as evident in the spectra of the colloid, and we conclude that its concentration is less than that of T4.

We do observe small intensity differences and peak shifts in the amide III region (1200–1400 cm^{-1}). This region is known to be sensitive to protein conformation as well, and particularly sensitive to the side chains and glycosylation[28] of the peptide backbone. However, since the changes in amide III patterns are concomitant with those in the amide I region, we cannot conclude whether there are any changes in thyroglobulin glycosylation in the colloids of normal patients.

Finally, we compare in Fig. 5 the spectra of follicular cells with those of colloid regions in direct contact with these cells. The follicular cells (blue trace, Fig. 5) display spectra quite similar to those of other glandular cells, although they exhibit slightly more prominent β-sheet signatures (1692 cm^{-1}). The collection of these spectra is quite difficult since these cells occur in a monolayer of cells *ca.* 10 μm thick.

The green trace in Fig. 5 shows the mean spectra from all colloid regions in the dataset. When compared to the mean follicular cell spectrum they appear quite similar, including the shape of the amide I band. Therefore, the mean spectrum from follicular cells is heavily dominated by the contribution of thyroglobulin. In the spectra of the follicular cells, a shoulder at 1610 cm^{-1} is observed that is associated with the amino acid tyrosine.[29] The amount of tyrosine in the follicular cells is high because the transcription of thyroglobulin requires a high amount of this amino acid.[30]

Conclusions

In this report, we present the spectral characterization of normal thyroid tissue as well as the FTIR spectra of thyroid hormones. The data processing methods applied in this paper enabled the acquisition and subsequent analysis of small follicular cells of thyroid tissue. This methodology will be applied in future studies in abnormal thyroid tissue. We show that SHP can be used to identify the amount of iodinated thyroglobulin present within the thyroid tissue.

Acknowledgements

Support of this work from CEPID/FAPESP 05/51689-2; Instituto Nacional de Fotônica/CNPq 573916/2008-0; CAPES/9036-11-3, CNPq 555621/2009-0 and 308277/2009-0 is gratefully acknowledged.

References

1 A. C. G. a. J. E. Hall, *Textbook of medical physiology*, Elsevier Saunders, Philadelphia, 2006.
2 C. S. B. Teixeira, R. A. Bitar, H. S. Martinho, A. B. O. Santos, M. A. V. Kulcsar, C. U. M. Friguglietti, R. B. da Costa, E. A. L. Arisawa and A. A. Martin, *Analyst*, 2009, **134**, 2361–2370.
3 V. K. R. S. Cotran, T. Collins and S. L. Robbins, *pathologic basis of disease*, Saunders, philadelphia, 1999.
4 L. C. U. Junqueira, J. Carneiro and A. N. Contopoulos, in *A Concise medical library for practitioner and student*, Lange Medical Publications, Los Altos, Calif., 1975, p. v.
5 D. Kirsten, *Neonatal Netw. J. Neonatal. Nurs.*, 2000, **19**, 11–26.
6 C. Yarrington and E. N. Pearce, *J. Thyroid Res.*, 2011, **2011**, 934104.
7 B. Bird, M. Miljkovic, M. J. Romeo, J. Smith, N. Stone, M. W. George and M. Diem, *BMC Clin. Pathol.*, 2008, **8**, 8.
8 B. Bird, K. Bedrossian, N. Laver, M. Miljkovic, M. J. Romeo and M. Diem, *Analyst*, 2009, **134**, 1067–1076.
9 J. M. Schubert, A. I. Mazur, B. Bird, M. Miljkovic and M. Diem, *J. Biophotonics*, 2010, **3**, 588–596.
10 T. Pereira, M. Dagli, G. Mennecier and D. Zezell, *Spectroscopy*, 2012, **27**, 399–402.
11 M. Diem, M. Miljkovic, B. Bird, T. Chernenko, J. Schubert, E. Marcsisin, A. Mazur, E. Kingston, E. Zuser, K. Papamarkakis and N. Laver, *Spectroscopy*, 2012, **27**, 463–496.
12 S. Boydston-White, M. Romeo, T. Chernenko, A. Regina, M. Miljkovic and M. Diem, *Biochim. Biophys. Acta, Biomembr.*, 2006, **1758**, 908–914.

13 B. Bird, M. Romeo, N. Laver and M. Diem, *J. Biophotonics*, 2009, **2**, 37–46.
14 Y. Liu, Y. Xu, Y. Zhang, D. Wang, D. Xiu, Z. Xu, X. Zhou, J. Wu and X. Ling, *Br. J. Surg.*, 2011, **98**, 380–384.
15 X. Zhang, Y. Xu, Y. Zhang, L. Wang, C. Hou, X. Zhou, X. Ling and Z. Xu, *J. Surg. Res.*, 2011, **171**, 650–656.
16 Y. Q. Liu, Y. Z. Xu, Q. G. Sun, X. Q. Zhang, Z. Xu, Y. F. Zhang, J. G. Wu, X. S. Zhou and X. F. Ling, *Zhonghua Zhongliu Zazhi*, 2009, **31**, 908–910.
17 C. S. B. Teixeira, R. A. Bitar, A. B. O. Santos, M. A. V. Kulcsar, C. U. M. Friguglietti, H. S. Martinho, R. B. da Costa and A. A. Martin, *Evaluation of thyroid tissue by Raman spectroscopy*, San Francisco, CA, 2010.
18 C. P. Schultz, K. Z. Liu, E. A. Salamon, K. T. Riese and H. H. Mantsch, *J. Mol. Struct.*, 1999, **481**, 369–377.
19 M. Miljkovic, B. Bird and M. Diem, *Analyst*, 2012, **137**, 3954–3964.
20 NIST- Standard Reference Data Program, 3,5-Diiodo-L-tyrosine. http://webbook.nist.gov/cgi/cbook.cgi?ID=300-39-0, accessed on 10 July 2013.
21 R. M. S. Alvarez, R. N. Farias and P. Hildebrandt, *J. Raman Spectrosc.*, 2004, **35**, 947–955.
22 K. Sorimachi and N. Ui, *Biochim. Biophys. Acta*, 1974, **342**, 30–40.
23 J. Handl, W. Kuhn and R. D. Hesch, *J. Endocrinol. Invest.*, 1984, **7**, 97–101.
24 M. Hansson, G. Berg and M. Isaksson, *X-Ray Spectrom.*, 2008, **37**, 37–41.
25 M. Hansson, T. Grunditz, M. Isaksson, S. Jansson, J. Lausmaa, J. Molne and G. Berg, *Thyroid*, 2008, **18**, 1215–1220.
26 B. Bird, M. S. Miljkovic, S. Remiszewski, A. Akalin, M. Kon and M. Diem, *Lab. Invest.*, 2012, **92**, 1358–1373.
27 S. Formisano, C. Moscatelli, R. Zarrilli, B. Diieso, R. Acquaviva, S. Obici, G. Palumbo and R. Dilauro, *Biochem. Biophys. Res. Commun.*, 1985, **133**, 766–772.
28 A. Barth, *Biochim. Biophys. Acta, Bioenerg.*, 2007, **1767**, 1073–1101.
29 A. Barth, *Prog. Biophys. Mol. Biol.*, 2000, **74**, 141–173.
30 D. Kirsten, *Neonatal Netw. J. Neonatal. Nurs.*, 2000, **19**, 11–26.